

exponentially rapidly, this being the emission threshold. Even here, however, the real part is relatively smooth. For weak coupling, the $m\nu^2$ term in $\text{Re}Z_\nu$ dominates; for stronger coupling, $\text{Re}Z_{\omega_0}/\text{Im}Z_{\omega_0} \approx \beta^{1/2}$, $\nu = \omega_0$. Thus $|Z_\nu|^2$ can be taken to be relatively smooth compared to

$X(\nu, n, \beta^{1/2}\sqrt{C'})$.

$^{17}Z_\pm(\nu)$ here is to be distinguished from $\overline{Z}_\pm(\nu)$ in Appendix B. No confusion should arise from this.

¹⁸J. W. Hodby, J. A. Borders, and F. C. Brown, J. Phys. C **3**, 335 (1970).

Magnetoresistance of Very Pure Polycrystalline Aluminum[†]

F. R. Fickett

National Bureau of Standards, Boulder, Colorado 80302

(Received 31 August 1970)

The behavior of the resistance of polycrystalline aluminum wires as a function of magnetic field and purity at temperatures of 4, 15, and 19.6 K is reported. Both longitudinal and transverse configurations were measured. The residual resistance ratios of the specimens varied from 1600 to 31 000. The measured magnetoresistance ($\Delta R/R_0$) is separated into a saturating and a linear part. The value of the saturating component is high at 19.6 K but is shown to be less than 6, even in the limit of infinite specimen purity. The linear component varies with both temperature and purity. Possible sources for the large saturating magnetoresistance values and for the variations observed in the linear portion are discussed. An analysis scheme is presented which allows prediction of the saturating component from zero-field resistance values. A deviation from Matthiessen's rule observed here, and by several other experimenters, is presented and discussed.

I. INTRODUCTION

The magnetoresistance of aluminum has been studied extensively.¹⁻⁵ Both single- and polycrystalline specimens have been measured. Most of the measurements were made only at 4 K on specimens of relatively low purity. Frequently, the specimens used were very small in at least one dimension, leading to the possibility of size effects. Several experiments, however, have been performed on large high-purity specimens and at temperatures up to 20 K.^{6,7} These measurements indicate that the magnetoresistance ($\Delta R/R_0$) rises dramatically with temperature, reaching as much as four times the value measured at 4 K.

The experiment reported here was designed to cover a range both of temperature (4–20 K), and of specimen purity [residual resistance ratio (RRR) = 1000–30 000]. Magnetoresistance measurements were made both in the transverse and longitudinal configurations. We hoped, by this technique, to arrive at a phenomenology which would characterize the magnetoresistance of aluminum, at least in the form of polycrystalline wires, over this range.

It has become almost axiomatic that the more simple metals, in the free-electron sense, exhibit magnetoresistance effects which are at odds with theory.⁸ Aluminum,¹⁻⁷ indium,⁹ potassium,¹⁰ and sodium¹⁰ all show a linear magnetoresistance at high fields. A typical curve for aluminum is shown in Fig. 1. Furthermore, no simple metal which

has been investigated over a wide range of purity and temperature has been observed to obey Kohler's rule. This indicates that the relative effects of different scattering mechanisms are more complex than the rule anticipates. More recent theoretical treatments such as those by Young,^{11,12} and Pippard,¹³ although promising some success in particular cases, have not yet shown wide applicability.

The Fermi surface of aluminum is well known and theoretical calculations of the major features have been adequately confirmed by de Haas-van Alphen and other experiments.¹⁴ In one instance, transverse-magnetoresistance rotation diagrams for several crystal orientations were calculated, based on early models of the surface; however, agreement with available experimental data was not good.¹⁵

Recently, a good deal of discussion has taken place as to the presence or absence of magnetic breakdown effects which could lead to extended orbits on the Fermi surface.^{7,13,14,16} The situation is still not totally clear, but it seems that magnetic breakdown may well occur in aluminum with the field along the $\langle 100 \rangle$ direction.

An extended orbit configuration, whatever its cause, would be expected to lead to a significant anisotropy of single-crystal transverse-magnetoresistance rotation diagrams. Early experiments showed no such large anisotropy,² whereas more recent work on higher-purity aluminum⁷ does show a considerable effect.

Finally, the creation of a significant linear mag-

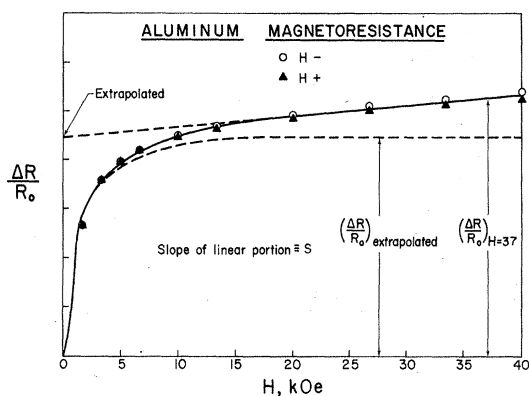


FIG. 1. General behavior of the magnetoresistance and definition of terms.

netoresistance in a polycrystalline specimen by the proper combination of crystallites with quadratic and saturating magnetoresistance does not appear likely, even in metals known to have open orbits.¹⁷

The remainder of the paper is constructed as follows. Section II describes the specimen preparation and the electrical measurements. A discussion is included on size-effect corrections. The experimental results are presented in Sec. III. Section IV gives a description of the analysis and a discussion of the results. Finally, Sec. V presents our conclusions and some suggestions for further work.

II. TECHNIQUES

A. Magnet, Dewar, and Voltage Detection Systems

The magnet used for these measurements is a conventional superconducting solenoid with a 1-in. bore. The maximum field used was 40 kOe. The field homogeneity is 0.5% over the specimen region.

Voltages are detected with a dc system described in an earlier publication.¹⁸ The system detects signals at the nanovolt level with an imprecision of 50 picovolts. It can operate at levels as high as 500 nV and in the presence of microvolt thermals. Specimen current was chosen to give a signal level near 50 nV, an optimum value for the detection system, in all cases where this was possible. The current ranged from 10 to 500 mA, depending on the specimen measured and the temperature. In all cases measurements of current dependence of the resistance with the magnet off confirmed that magnetoresistive effects of the specimen current were negligible.

An isolation Dewar within the magnet bore contains the cryogenic fluid, hydrogen or helium. This Dewar can be pumped for temperature control. The specimen, enclosed in a vacuum can with a low pressure of helium gas for heat transfer, is

immersed in the cryogen and centered in the magnet bore. A system of gear-driven push rods is used to align the specimen with respect to the magnetic field.

B. Specimens

Table I gives a summary of several properties of the specimens. Figure 2 shows the mounting configuration. The tight winding of the transverse specimen on the aluminum form is made necessary by the small magnet bore. The longitudinal specimen is attached with varnish to an aluminum pallet for the measurements.

The slugs for the wires are prepared from the bulk material by compressing to ~0.1-in.-thick plate, sectioning into strips, chemically cleaning, annealing, and finally swaging to the desired diameter. The wires are chemically cleaned and annealed after passing through every other die. The cleaning solution used (70% H₃PO₄, 25% H₂SO₄, 5% HNO₃) will give either an etch (2 min at 60 °C) or a polish (seconds at 100 °C). The final treatment of the specimens varies; some low-purity specimens are etched, some polished. All high-purity specimens are etched. The anneal procedure is the same in all cases, 1 h at 300 °C and a furnace cool. The transverse specimens are given a final anneal after winding.

The longitudinal and transverse specimens of a given purity are not necessarily from the same wire, as is indicated by their designation. In the instances where the two specimens are from the same wire and of high purity (4.0-T, L of the table and several not reported here), the winding of the transverse specimen caused a slight (<10%) increase in its residual resistance. The cause of this increase appears to be a slight offsetting of the rather large grains during winding. Grain diameter in wires Nos. 3 and 4 tends to be 1–2 mm; the less pure wires have significantly smaller grains.

The wire processing described, exclusive of the winding, maintains the purity of the bulk material for all purities except the highest. The purity of the bulk aluminum is measured by an eddy current decay method before processing is begun. The highest-purity aluminum has an eddy current ratio near 35 000. Our dc measurement gives 31 000 in the wire. Errors in the two different size-effect corrections involved are such that the difference may not be meaningful.

Copper current caps are lightly crimped to the wires and filled with a low-melting-point solder. The current leads are then soldered into the caps. Potential leads of No. 36 copper wire are looped around the specimen, twisted and the joint is covered with conducting epoxy. This type of contact has proven to be reliable on repeated cycling from room temperature to 4 K and results in minimum

3 MAGNETORESISTANCE OF VERY PURE POLYCRYSTALLINE ALUMINUM 1943

TABLE I. Specimen data summary. Resistivity is determined by calculating A/L from the room-temperature resistance and the value $\rho(295\text{ K}) = 2.74\ \mu\Omega\text{ cm}$.

| Designation ^a | Diameter (mm) | T (K) | Measured $R(\mu\Omega)$ | Measured $\rho(10^{-4}\ \mu\Omega\text{ cm})$ | Size correction $\rho_{\text{measured}}/\rho_{\text{corr}}$ |
|--------------------------|---------------|-------|-------------------------|---|---|
| 1.0-T-2 | 0.94 | 4 | 6.42 | 14.0 | 1.06 |
| | | 15 | 8.85 | 19.4 | 1.04 |
| | | 19.6 | 11.42 | 25.0 | 1.03 |
| 2.0-T-6 | 0.89 | 4 | 3.32 | 5.55 | 1.16 |
| | | 15 | 5.23 | 8.74 | 1.10 |
| | | 19.6 | 7.58 | 12.7 | 1.07 |
| 3.1-T-14 | 1.55 | 4 | 0.482 | 2.36 | 1.24 |
| | | 15 | 0.994 | 4.86 | 1.10 |
| | | 19.6 | 1.72 | 8.42 | 1.06 |
| 4.0-T-28 | 1.52 | 4 | 0.268 | 1.43 | 1.47 |
| | | 15 | 0.658 | 3.52 | 1.15 |
| | | 19.6 | 1.27 | 6.81 | 1.07 |
| 1.1-L-2 | 1.66 | 4 | 0.123 | 17.6 | 1.02 |
| | | 15 | 0.159 | 22.7 | 1.02 |
| | | 19.6 | 0.197 | 28.1 | 1.02 |
| 2.0-L-5 | 0.89 | 4 | 0.157 | 5.81 | 1.16 |
| | | 15 | 0.250 | 9.26 | 1.09 |
| | | 19.6 | 0.363 | 13.4 | 1.06 |
| 3.0-L-16 | 1.40 | 4 | 0.0238 | 2.26 | 1.28 |
| | | 15 | 0.0527 | 5.00 | 1.11 |
| | | 19.6 | 0.0897 | 8.50 | 1.06 |
| 4.0-L-31 | 1.52 | 4 | 0.0105 | 1.34 | 1.52 |
| | | 15 | 0.0278 | 3.54 | 1.15 |
| | | 19.6 | 0.0554 | 7.06 | 1.07 |

^aSpecimen designation scheme for, say, 3.1-T-14, would be lot No. 3, wire No. 1, configuration T, and a RRR of 14 (in thousands).

damage to the specimen.

C. Magnetoresistance Measurements

The magnetoresistance voltage measurement is straightforward. The field is stationary for each measurement and each point represents an average containing reversal of both specimen current and field.

Specimen alignment is not considered as critical here as in single-crystal measurements¹⁹ and our alignment of the axis of the transverse form and of the longitudinal specimens with respect to the field has about a 1° maximum error. The use of the spiral winding for the transverse specimen introduces a uniform 4° deviation from proper alignment, even when the axis of the form is accurately parallel to the field. Since the transverse specimens are much less sensitive to misalignment effects than the longitudinal ones, we feel this error does not significantly affect the results.

D. Size-Effect Corrections

The measured zero-field resistance for each specimen is given in Table I. The resistivity is determined by calculating A/L from the room-

temperature resistance using Meaden's²⁰ value $\rho(295\text{ K}) = 2.74\ \mu\Omega\text{ cm}$. This number and the measured resistance at the temperature of interest are then used to compute the resistivity.

The zero-field resistivity must be corrected for the size effect. The longest electron mean free paths calculated for our specimens are on the order

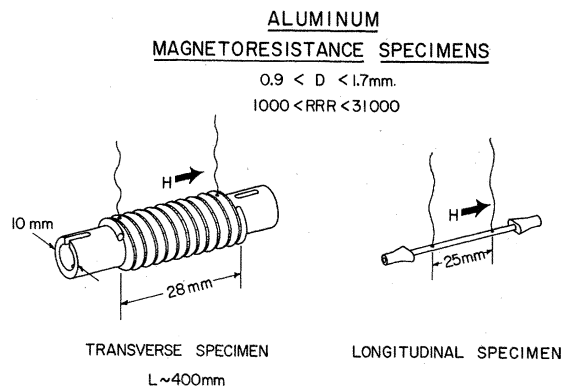


FIG. 2. Specimen description and mounting configuration.

of 1 mm, so that l/d is never greater than 1 (d is the specimen diameter shown in Table I). Nevertheless, the surface-scattering contribution to the resistivity ranges from 2 to 52% of the bulk resistivity, as shown in Table I. It is obvious that corrections of this magnitude will be significant in determining the bulk magnetoresistance values, and yet they are often either ignored or described in too little detail.²¹ This point becomes especially critical when one attempts to compare data from many sources. Much of the available magnetoresistance data on aluminum comes from measurements on much smaller specimens than ours, yet in many instances one cannot tell whether or not a correction has been made, much less which correction scheme was used. For this reason we use the superscript c to indicate corrected data.

The general problem of size-effect resistivity is reviewed by Brandli and Olsen.²² Specific applications to aluminum have been made by Corruccini²¹ and by Arp *et al.*²³ Figure 10 of the latter paper shows a comparison of the theories of Fuchs, Soffer, and Parrot-Cotti. This graph indicates that all the theories are essentially in agreement at values of $l/d < 1$ with the exception of the (probably) unrealistic case of total specular reflection. Furthermore, the correction resulting from these theories does not differ by more than a few percent from the result of the simple Nordheim formula

$$\rho_{\text{bulk}} = \rho_{\text{measured}} - (\rho l)_{\text{bulk}}/d. \quad (1)$$

This formula is used for all corrections in this paper. This scheme, and most of the others, requires a knowledge of the quantity $(\rho l)_{\text{bulk}}$, a number that is not at all certain. Brandli and Olsen quote values ranging from 0.35 to $0.88 \times 10^{-11} \Omega \text{ cm}^2$. We use the value

$$(\rho l)_{\text{bulk}} = 0.7 \times 10^{-11} \Omega \text{ cm}^2$$

as representing a reasonable average of values reported in the helium-temperature range.²³ This number, along with the measured resistivity, is also used to determine approximate mean-free-path values.

The same size-effect correction is used for the 15 and 20-K data, although $(\rho l)_{\text{bulk}}$ is not expected to be temperature independent. We feel this will represent a good first approximation and, in any event, the relative effect of the correction decreases with increasing temperature. Obviously, good experimental measurements of this quantity as a function of purity and temperature are needed.

We recognize that the application of a transverse magnetic field does not remove, essentially, all surface scattering as does a longitudinal field.²² However, there is no good theory to cover this case

and the effect may well be small; thus, we assume here that it is not necessary to correct the high-field data.

III. RESULTS

Figure 1 explains the terminology to be used in the remainder of the paper. A superscript c is added to data which have been corrected for size effect. The rest of the terminology is conventional. RRR designates the residual-resistance ratio measured to room temperature, $R(295 \text{ K})/R(4 \text{ K})$. $RR(T)$ is the ratio between the room-temperature resistance and the resistance at T . No correction is made for thermal contraction of the specimens since this correction is much smaller than the expected error in the size-effect correction.

A. Zero-Field Resistivity

A strong deviation from Matthiessen's rule is shown by our rather limited data. The observed behavior is illustrated in Fig. 3, where we have plotted $\rho(20.4 \text{ K}) - \rho(4 \text{ K})$ as a function of purity. We expect this quantity to be a measure of the intrinsic resistivity, and thus independent of purity. This type of behavior was also reported by Borovik *et al.*,⁶ and their data as well as data from several other sources^{1,24-26} are presented in the figure. The errors associated with most of the points are unknown but are expected to be quite large, particularly at lower purities. Our data has been corrected to 20.4 from 19.6 K, using $\rho(20.4 \text{ K})/\rho(19.6 \text{ K}) = 1.227$ derived from the Bloch-Grüneisen calculation of Pawlek and Rogalla.²⁴ Their calculation, which assumes $\theta_D = 408 \text{ K}$, is also used to determine the Bloch-Grüneisen value of the intrinsic resistivity at 20.4 K, which is shown as the dashed

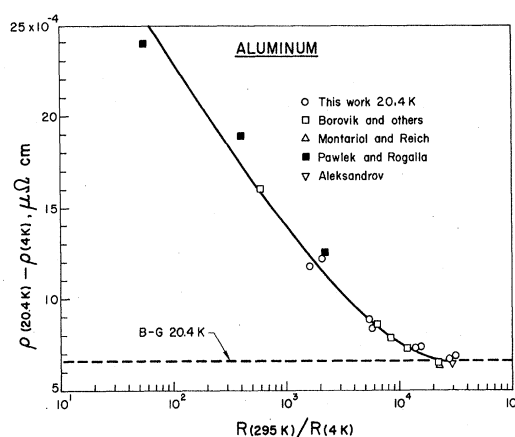


FIG. 3. Deviation from Matthiessen's rule as a function of purity. Our data, taken at 19.6 K, has been adjusted to 20.4 K as described in the text. The horizontal line represents the intrinsic resistivity at 20.4 K as derived from a Bloch-Grüneisen calculation.

horizontal line in Fig. 3.

B. Transverse Magnetoresistance

Representative transverse-magnetoresistance curves are shown in Fig. 4. The relative imprecision of the data is less than 1%. The low-field magnetoresistance is not shown in detail but measurements on the magnetoresistive effect of the specimen current discussed earlier show it to be quadratic with field.

Since essentially all of the magnetoresistance curves are of the form shown in Fig. 1, we separate them into a saturating portion and a linear portion for analysis. This is done, as shown, by extrapolating the high-field linear magnetoresistance to zero field and subtracting.

The data are summarized in Fig. 5. The abscissa is the corrected resistance ratio (RR) at the temperature of measurement $R(295 K)/R(T)$. At each temperature the lower line represents the behavior of the saturating portion of the magnetoresistance and the upper line represents the behavior of the complete magnetoresistance, including the linear portion at 40 kOe. The error bars here are relatively large because different specimens are being compared and the error in the size-effect correction, and thus in the resistivity calculation,

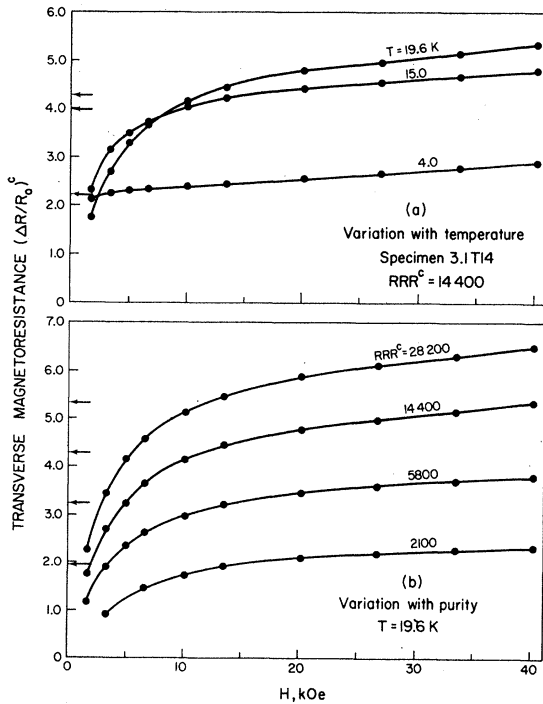


FIG. 4. Transverse-magnetoresistance data. The zero-field resistance has been corrected for size effect. The arrows at $H=0$ show the extrapolated intercept of the linear region for each curve. This is the saturation value used for Figs. 5 and 6.

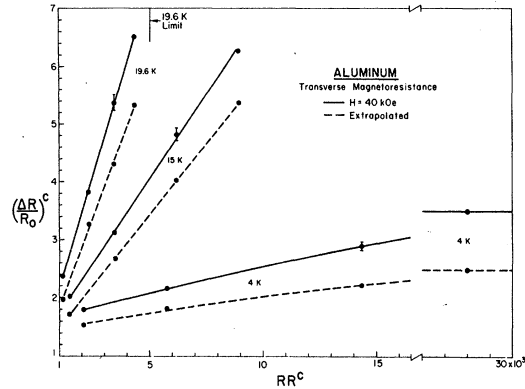


FIG. 5. Summary of transverse-magnetoresistance data. Note the break in scale on the abscissa, $RR(T) \equiv R(295)/R(T)$. The 4-K curve has been drawn level at the highest purity; the actual behavior is uncertain. More data is needed in the 15 000–30 000 range. The 19.6-K limit shown is from the intrinsic resistivity as calculated by Pawlek and Rogalla.

tion, must be taken into account. That all points at a given temperature and field should fall on straight lines was unexpected. The 4-K curve may be an exception – we have drawn the curve level beyond the axis break to indicate this possibility.

The 19.6-K limit shown in Fig. 5 is the RR derived from the calculated intrinsic resistivity at this temperature.²⁴ Deviations from Matthiessen's rule are ignored. This value determines the maximum limit of the magnetoresistance at a given temperature, i. e., the limit of infinite metallic purity.

A more conventional presentation of the saturation data is made in Fig. 6. There are only three data points to a curve and thus the curves indicated

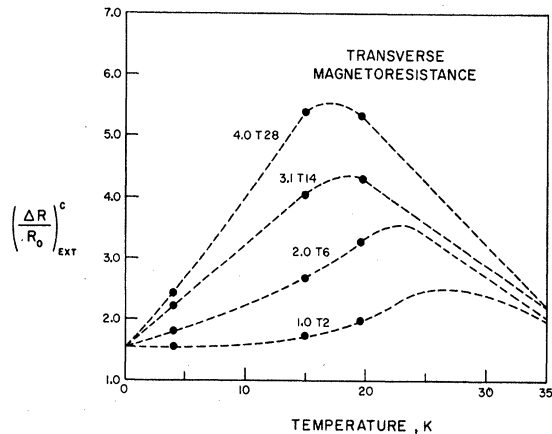


FIG. 6. Saturation value of the transverse magnetoresistance plotted as a function of temperature. The dashed lines are only intended to show a possible set of curves. There are no data above 20 K.

by the dashed lines are meant only to be suggestive of a possible behavior. Note that this behavior is also shown in Fig. 6 of the paper by Chiang *et al.*,⁷ over the range 4–22 K. At either end of the plot we expect that a single isotropic scattering mechanism is operative. This is in contrast to the central portion where small-angle phonon scattering can be expected to play an important role. At high temperatures, the rapid increase of R_0 drops the value of $\Delta R/R_0$. At very low temperatures, a convergence of the curves is shown which is consistent with the analysis presented in Sec. IV.

Lest the wrong conclusion be drawn from the high magnetoresistance values presented in Figs. 5 and 6, we show a plot in Fig. 7 of the actual resistivity at 40 kOe as a function of purity at various temperatures. Note that, even where we have a dramatic increase of $\Delta R/R_0$ with purity, the corresponding decrease of the zero-field resistance is more than sufficient to result in a lower actual resistivity for the higher-purity specimens.

C. Longitudinal Magnetoresistance

In general the longitudinal-magnetoresistance data is similar in form to the transverse. Representative curves are shown in Fig. 8. The longitudinal-magnetoresistance values are smaller than the transverse values for specimens of nearly the same purity. This is the situation one would expect both from theory and from results on other metals.⁸

The data are summarized in Fig. 9, identical in construction to Fig. 5. A smaller amount of data is shown here, but the behavior appears to be the same as that shown by the transverse magnetoresistance.

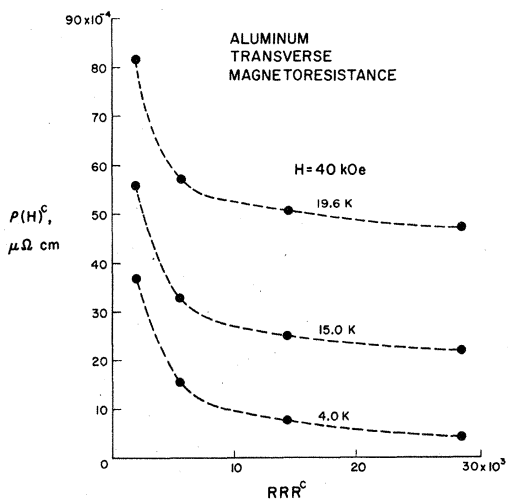


FIG. 7. Actual resistivity of aluminum specimens vs purity at 40 kOe.

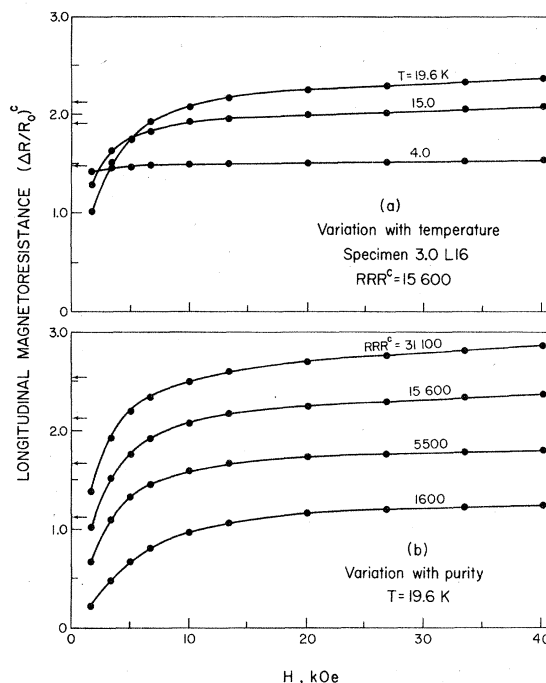


FIG. 8. Longitudinal-magnetoresistance data. The zero-field resistance has been corrected for size effect. The arrows at $H=0$ show the extrapolated intercept of the linear region for each curve. This is the saturation value used for Fig. 9.

D. Anomalous Longitudinal Magnetoresistance

The magnetoresistance curve at 4 K for the highest-purity longitudinal specimen (4.0-L-31) is not of the form shown in Fig. 1. The magnetoresistance rises in the normal manner, appears to approach saturation at a very low value, and then rises roughly as $H^{1.6}$ to the highest field measured. These data are not included in the analysis. The source of the observed behavior is discussed further in Sec. IV.

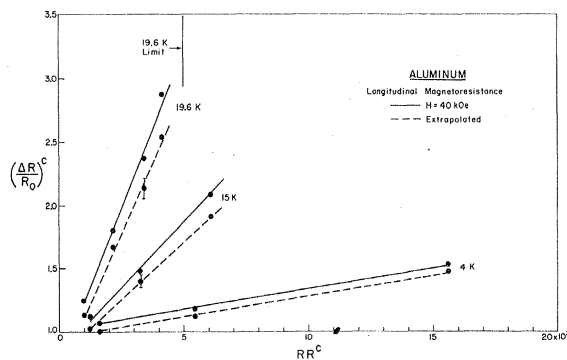


FIG. 9. Summary of longitudinal-magnetoresistance data. The 19.6-K limit shown is from the intrinsic resistivity as calculated by Pawlek and Rogalla.

IV. DISCUSSION

A. Zero-Field Resistivity

The type of deviation from Matthiessen's rule shown in Fig. 3 is not unique to aluminum. Neighbor and Newbower²⁷ have recently published a study on indium in which they see a behavior similar to that observed here. The temperature range of their observations is lower than that for aluminum, consistent with the lower Debye temperature. The Fermi surfaces of these two metals are qualitatively identical.²⁸ On the other hand, when we plot copper data over three orders of magnitude of purity, we find no significant variation of this type. To the accuracy of the data, $\rho(20\text{ K}) - \rho(4\text{ K})$ is a constant for copper.

Deviations from Matthiessen's rule have been observed in many other experiments on aluminum and many mechanisms have been proposed as the villain; among these, strain, impurity content, and surface scattering. Figure 3 shows such a consistency over so many specimens from such diverse sources that one is led to suspect that a bulk mechanism of some sort is responsible.

B. Saturating Component of Magnetoresistance

The relatively high magnetoresistance observed at 15 and 20 K is apparently a property of the saturating component and is not due to the existence of a linear portion. Similar results have been reported for copper²⁹ and are consistent with a small-angle scattering theory. The Fermi surface of aluminum does not offer the same possibilities for large effects at the onset of small-angle scattering as does copper with its large neck regions. A means by which small-angle effects might give significant contributions to the magnetoresistance of aluminum has been discussed in detail by Pippard.¹³ The small size of the regions of the surface which can contribute seems to indicate that this mechanism alone is not likely to be the explanation of the high magnetoresistance, particularly in polycrystalline materials or in a longitudinal configuration. A somewhat different approach has been proposed by Young *et al.*³⁰ which is basically an impurity-assisted small-angle scattering mechanism resulting in intersheet scattering. Calculations from this model were quite successful in explaining the magnetoresistance data of Katyal and Gerritsen³¹ on cadmium. Many variations of magnetoresistance and Hall resistivity are possible, depending on the choice made for the intersheet scattering parameter. In the case of polycrystalline aluminum, however, it seems that the increase of magnetoresistance with temperature and the uniform field dependences observed argue against using such a mechanism to explain the bulk magnetoresistance.

Magnetic breakdown, as mentioned earlier, has been considered as possibly responsible for the observed magnetoresistance. Again, breakdown only appears to be likely for a $\langle 100 \rangle$ crystal direction¹⁶ affecting only a small number of electrons, although Chiang *et al.*⁷ have recently postulated its existence over a wider area of the Fermi surface. Falicov and Sievert³² have calculated the magnetoresistance for several breakdown situations which could apply to aluminum orbits. The results for breakdown orbits on the second zone hole surface (Fig. 11 of Ref. 30) have been cited by Chiang *et al.*⁷ as responsible for their observed single-crystal saturation data. Our observation that the behavior of the longitudinal and transverse magnetoresistances is qualitatively the same, together with the extreme variations observed with temperature and purity for the magnetoresistance of polycrystalline specimens, suggests that here breakdown is not the major explanation.

Perhaps the most promising of the current theoretical approaches is that taken by Young in which umklapp-process "hot spots" provide a channel by which electrons can be rapidly removed from the conduction process.¹¹ It is possible that this mechanism could combine with small-angle scattering to give the observed large magnetoresistance in the small-angle scattering region. Detailed calculations have not been made for aluminum but Young suggests that this mechanism can give both inter- and intraband scattering. In light of the results presented here, it seems that such calculations would be worth pursuing. Certainly the consistent behavior with temperature shown in Figs. 5 and 9 is a very convincing argument for the presence of a phonon effect on the magnetoresistance. Furthermore, the apparent tendency of the 4-K curve of Fig. 5 to become independent of purity at high values of RRR and its low slope indicate the lack of a significant magnetoresistance effect due solely to removal of impurities. In other words, Kohler's rule is not obeyed.

Figures 5 and 9 suggest an interesting analysis scheme. We assume that the measured saturation magnetoresistance, be it transverse or longitudinal, can be separated into a phonon part and an impurity part. We further assume that these two parts combine with the zero-field resistance to give the magnetoresistance in the following manner:

$$\frac{\Delta\rho}{\rho_0} \Big|_{\text{measured}} = \frac{\Delta\rho_{\text{phonon}} + \Delta\rho_{\text{impurity}}}{\rho_{\text{measured}}} \quad (2)$$

The separate $\Delta\rho$ terms are computed from the data of Figs. 5 and 9 as follows:

Phonon part. The straight line representing the saturation data at a given temperature is drawn to intersect a vertical line representing infinite purity

at that temperature. The value of RR at which this vertical line is drawn is determined from a Bloch-Grüneisen (B-G) calculation as discussed earlier. Then,

$$\Delta\rho_{\text{phonon}} = \left. \frac{\Delta\rho}{\rho} \right|_{\text{limit}} \rho_{\text{B-G}}. \quad (3)$$

This term is independent of impurity type or concentration; it depends only on temperature.

Impurity part. We assume that

$$\rho(4\text{ K})_{\text{measured}} = \rho_{\text{impurity}}. \quad (4)$$

Using this value in the denominator of Eq. (2), and the 4-K $\Delta R/R_0$ data, we find $(\Delta\rho/\rho)_{\text{impurity}}$. For this calculation, a linear fit to the 4-K data is used. We assume that this $(\Delta\rho/\rho)_{\text{impurity}}$ is a constant independent of impurity type or concentration and independent of temperature. The presence of transition-metal impurities might well change these assumptions. Clearly,

$$\Delta\rho_{\text{impurity}} = \left. \frac{\Delta\rho}{\rho} \right|_{\text{impurity}} \rho(4\text{ K})_{\text{measured}}. \quad (5)$$

Both of the quantities in the numerator of Eq. (2) depend on the measurement configuration, longitudinal or transverse. Note also that

$$\rho(T)_{\text{measured}} \geq \rho(T)_{\text{B-G}} + \rho_{\text{impurity}}, \quad (6)$$

as indicated in Fig. 3.

When this scheme is applied to the data of Figs. 5 and 9, we derive the values shown in Table II for the various terms. These values inserted in Eq. (2) reproduce all of the data to within a few percent.

We would like to suggest that the numbers presented in Table II be considered as typical of aluminum, at least in polycrystalline form. To support this contention we present in Fig. 10 a plot showing transverse-magnetoresistance saturation data from several sources.^{1-3,6,15,33} This plot is Fig. 5 with our own data points removed but with the lines remaining.

TABLE II. Analysis values from Eq. (2). Separated contributions to the total magnetoresistance. Bloch-Grüneisen values for the phonon resistivity: $\rho_{4,0} = 2.3 \times 10^{-7} \mu\Omega \text{ cm}$; $\rho_{15,0} = 1.43 \times 10^{-4} \mu\Omega \text{ cm}$; $\rho_{19,6} = 5.41 \times 10^{-4} \mu\Omega \text{ cm}$.

| | T (K) | Transverse specimens | Longitudinal specimens |
|--|------------|-------------------------|---------------------------|
| $\left. \frac{\Delta\rho}{\rho} \right _{\text{impurity}}$ | All | 1.51 | 0.94 |
| $\left. \frac{\Delta\rho}{\rho} \right _{\text{phonon}}$ | 4.0 | 435 | 406 |
| | 15.0 | 10.2 | 4.23 |
| | 19.6 | 6.0 | 2.86 |

The data presented here are not necessarily corrected for size effect but, in most cases, the correction is expected to be small. Furthermore, only data plots where a linear portion could be identified, and subtracted, were used. In any case, for one reason or another, large errors are to be expected. The only usable data available in the literature above 4 K are those of Borovik and co-workers. These data are taken at 20.4 K, whereas the line drawn from our data is for 19.6 K, and thus the slightly higher slope which would be obtained for a linear fit to the Borovik data is to be expected. Chiang *et al.*⁷ give curves at 20 K, but the maximum field is not high enough to define the linear region well.

No similar plot is shown for the longitudinal magnetoresistance. Only one curve exists which might be used³⁴ and there is some question as to the actual purity of the specimen. The residual resistance ratio is given as 26000, but the stated impurity level of 2 ppm is more compatible with a ratio of 2600. If the latter ratio is the correct one, agreement with the 4-K line of Fig. 9 is excellent.

If we believe this analysis, there are two further interesting features to be considered: First, the additional resistance

$$\rho_{\text{add}} = \rho(T)_{\text{measured}} - [\rho(T)_{\text{B-G}} + \rho_{\text{impurity}}], \quad (7)$$

whatever its source, does not contribute significantly to the numerator of Eq. (2), i. e., is not field dependent. Second, addition of the linear component of the magnetoresistance (the curves at 40 kOe in Figs. 5 and 9) appears to affect the slope of the lines only slightly. This behavior indicates a relatively small effect on the phonon contribution to the magnetoresistance. The vertical displacement of the curve is most strongly related to the impurity magnetoresistance. Stated differently, the curves suggest that the *linear* portion of the magnetoresistance is the result of a slight phonon effect and a relatively large temperature-independent effect. This behavior is perhaps indicative of an impurity-assisted phonon scattering.^{30,35}

As a final step in the analysis of the saturation data, we determine the value of $\omega\tau$ at saturation. The calculation of ω is straightforward, assuming that the free-electron mass is used. The relaxation time τ is usually computed using some value of the quantity $(\rho l)_{\text{bulk}}$ from the literature and the measured resistivity ρ by

$$\tau = l/v_F = (\rho l)_{\text{bulk}} / \rho v_F, \quad (8)$$

where v_F is the free-electron Fermi velocity. Thus,

$$\omega\tau \propto (\rho l)_{\text{bulk}} \rho^{-1} H, \quad (9)$$

or, using our numbers

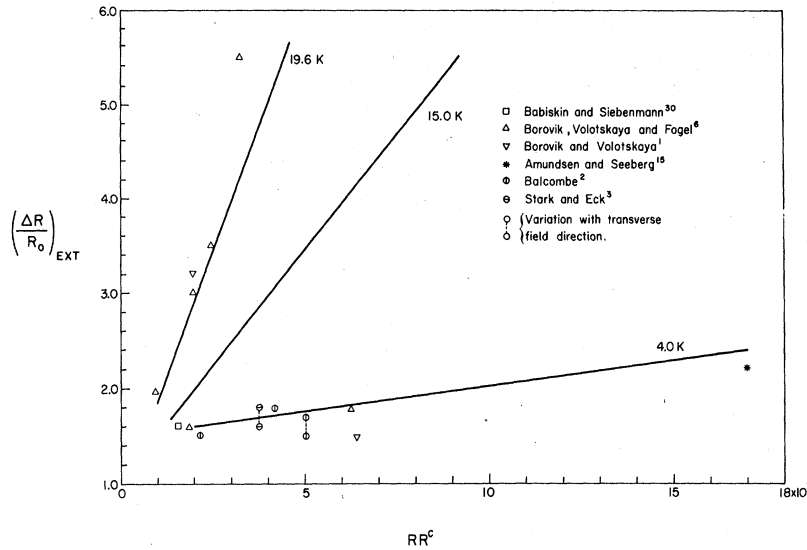


Fig. 10. Transverse-magneto-resistance data from the sources indicated. In each case the linear portion has been subtracted from the data shown in the papers referenced. The three lines represent our data from Fig. 5. The high-temperature data of Borovik *et.al.*, (Δ and ∇) was taken at 20.4 K, Balcombe's data (\odot) at 1.4K.

$$\omega \tau = 2.3 \times 10^{-4} \mathcal{R}_{RR(T)} H, \quad (10)$$

where H is in kOe ($1 \text{ Oe} = 79.58 \text{ A/m}$) and $\mathcal{R}_{RR(T)}$ is the value of RR at T .

To determine the value of $\omega \tau$ at saturation, we need only the value of H at that point. For this purpose we define the saturation point of a corrected magnetoresistance curve to be the point at which the linear component of the magnetoresistance and the measured magnetoresistance first coincide (see Fig. 1, $H_{\text{sat}} \approx 16 \text{ kOe}$). The location of this point is highly inaccurate due to the wide spacing of the data points but, even allowing for this error, the values found for $\omega \tau$ at saturation are not constant as one would expect from simple theory. We would like to suggest that the variation observed in the saturation value of $\omega \tau$ can be interpreted as being due to a variation of $(\rho l)_{\text{bulk}}$ and may, under proper circumstances, represent a relatively painless method of measuring this quantity. An examination of Eq. (9) shows that

$$\rho l|_{\text{bulk}} \propto \omega \tau|_{\text{sat}}^{-1}, \quad (11)$$

where now ρl is the variable and the right-hand side is the measured value of $\omega \tau$ at saturation. We have plotted this quantity as a function of specimen purity in Fig. 11. The bars represent the variation with temperature observed for a given specimen. This variation is not generally large and although the data suggest a minimum at 15 K, it is by no means certain. The variation with purity is more certain. Similar behavior has been observed in our work on copper²⁹ and in Strom-Olsen's³⁶ work on silver specimens. In both of those cases the electrical purity of the specimens was increased by an oxygen-anneal treatment. It appears likely that the changes shown in $(\rho l)_{\text{bulk}}$ with purity are

the result of changing effectiveness of the available impurity scattering centers.

A size-effect correction is applied to all the data of Fig. 11 and this correction involves a choice of $(\rho l)_{\text{bulk}}$ for the correction term. Thus, these data have some, usually relatively small, error from this source. An experiment on large specimens with say, $d/l > 10$, perhaps using superconducting voltage detection would prove much more definitive.

The above development is just one way of interpreting the experimental fact that the saturation of the magnetoresistance does not occur at any single value of $\omega \tau$ over a range of purity and temperature. Pippard¹³ has shown that, under the proper conditions, small-angle scattering can result in variations of $\omega \tau_{\text{sat}}$ and, it seems that, in fact, any mechanism, such as intersheet scattering³⁰ or magnetic breakdown,³² which allows alternate path orbits to combine with small-angle effects may give

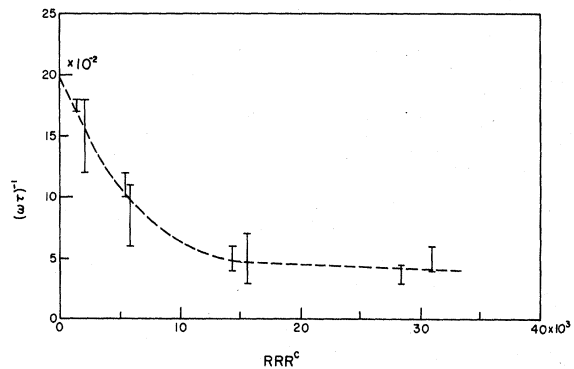


FIG. 11. Inverse of $\omega \tau$ as calculated at saturation field vs purity. The bar at a given purity covers the values found at 4, 15, and 19.6 K.

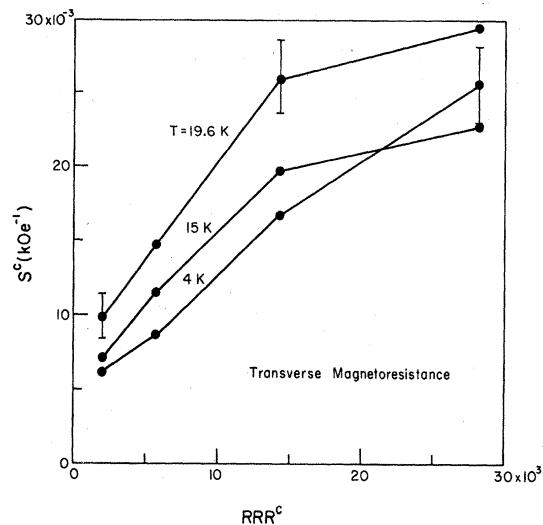


FIG. 12. Slope of the linear portion of the transverse magnetoresistance as a function of specimen purity and temperature. The errors shown are typical.

rise to similar behavior.

C. Linear Component of Magnetoresistance

The source of the linear component of the magnetoresistance observed in aluminum and other metals is one of the longer standing mysteries of metal physics. Proposed explanations of the behavior generally fall into two classes: bulk effects and finite-specimen effects. Within each class a number of mechanisms have been proposed and, usually, experimental evidence for the mechanism is presented. The discussion and references presented in Sec. I and earlier in this section cover most of the cases of interest.

This experiment offers some chance to look at gross variations of the slope values $\partial(\Delta\rho/\rho)/\partial H$ over a range of parameters. In spite of a low accuracy in slope determination, some correlations are observed which seem to be significant. The observed slopes are not large, varying from 0.001 to 0.030 kOe⁻¹. Linear portions are observed for all specimens in both the longitudinal and transverse configurations. The slopes tend to be higher for the transverse case, as does the saturating magnetoresistance. The transverse-magnetoresistance slope data is shown in Fig. 12. The correlations shown are also observed in the longitudinal data. The slope for a given specimen (fixed RRR) generally increases with temperature. At a given temperature, a strong increase of slope with purity is seen. The only exception is the 4-K longitudinal data where the slope decreases slightly as the purity increases.

The implication of this plot, in agreement with the discussion following Eq. (7), is that there is

both a bulk phonon mechanism and a bulk mechanism, which is temperature independent, active in the production of the linear region. Again, the temperature-independent part appears to be dominant. Also, unless a great deal of regularity is masked by the large errors, it seems that a relatively small contribution must exist which is related to surface treatment and history of specimen preparation. Thus there are three mechanisms which may contribute to the linear magnetoresistance, and definitive experiments will require very careful specimen preparation and characterization.

The relative sizes of these various effects may indicate why Balcombe,² with relatively impure (RRR ~ 3000) specimens, noticed no change in the magnetoresistance with surface treatment, whereas Amundsen and Seeberg³⁷ found the slope to be decreased significantly when the surface layer was etched from a high-purity (RRR ~ 17000) specimen. Further experiments on the effect of specimen characteristics due to methods of preparation are presently in progress.³⁸

D. Anomalous Magnetoresistance

The behavior exhibited by the highest-purity longitudinal specimen as described in Sec. IID is apparently another case of an anomalous voltage signal appearing on a single probe set due to a slight misorientation of a relatively short, very high-purity specimen from parallelism with the field. This effect is not uncommon and is discussed in detail in another paper.¹⁹ We do not feel that the data are significant in terms of bulk properties and thus only the 20-K data for specimen 4.0-L-31 is used in the analysis. A misorientation effect of this type is most likely responsible for the similar behavior observed by Balcombe and Parker¹⁶ in the longitudinal configuration, although their specimen purity was relatively low (RRR ~ 6000). Also, it seems likely that the extreme value of $\Delta R/R_0$ of 10 reported at 4 K by Borovik and Volotskaya¹ could have resulted from a similar effect in the transverse configuration. In support of this conjecture we note that recent extensive rotation diagrams on a large number of specimens of similar purity⁷ do not show any such large numbers at 4 K and no other investigators have reported numbers of this size.

V. CONCLUSIONS

High-purity aluminum exhibits significant deviations from Matthiessen's rule. The deviations appear to be largest at the lowest purities.

The magnetoresistance ($\Delta R/R_0$) of high-purity aluminum becomes large at temperatures in the liquid-hydrogen range. Large values are not observed at liquid-helium temperatures. The large values are a property of the saturating part of the

magnetoresistance. The origin of this behavior is not clear but a theoretical approach combining small-angle scattering with U -processes seems to be most promising. The observed temperature dependence indicates that the majority of the small-angle scattering interactions are due to phonons rather than to extended lattice defects.

The saturating component of the magnetoresistance can always be decomposed into a fixed-phonon part and a constant-impurity magnetoresistance. Variations in the observed magnetoresistance with purity at a given temperature then arise from the impurity resistivity and an additional zero-field resistivity which is impurity dependent but does not contribute significantly to the magnetoresistance numerator.

The actual resistivity in a magnetic field at a given temperature decreases with increasing purity, i. e., the opposite behavior of that observed for $\Delta R/R_0$.

The analysis and the graphs of Figs. 5 and 8 give a means of predicting to about 5%, the magnetoresistance at 4, 15, and 19.6 K of any relatively high-purity polycrystalline aluminum wire whose corrected RR is known. Temperatures intermediate to those measured can be handled with slightly lower accuracy by interpolation.

It is possible that magnetoresistance data can

be used to determine the variation of the quantity $(\rho l)_{\text{bulk}}$ with temperature and purity.

The origin of the linear portion of the magnetoresistance is unknown. The data suggest a combination of bulk and surface processes. In our case, bulk temperature-independent processes appear to be dominant.

Further measurements on large well-characterized single-crystal specimens are needed. Our experience with copper indicates that longitudinal-magnetoresistance measurements should be especially helpful in determining, and separating, the bulk magnetoresistance mechanisms. Also, the possibility exists, and should be investigated, that the addition of selected transition-metal impurities to high-purity aluminum might bring about a decrease in the magnetoresistance without a corresponding zero-field resistance increase.

ACKNOWLEDGMENTS

The high-purity aluminum was supplied by Dr. M. B. Kasen. W. German processed the aluminum into wire with great care. Thanks are due them and the rest of the cryogenic-properties-of-solids group for a continuing and stimulating exchange of ideas. Particular thanks are due Dr. A. F. Clark for his assistance in the formulation of many of the ideas presented here.

[†]This work was carried out at the National Bureau of Standards under the partial sponsorship of the U. S. Army Missile Command, Redstone Arsenal, Ala., and the U. S. A. E. C. Interlaboratory Committee.

¹E. S. Borovik and V. G. Volotskaya, Zh. Eksperim. i Teor. Fiz. 48, 1554 (1965)[Soviet Phys. JETP 21, 1041 (1965)].

²R. J. Balcombe, Proc. Roy. Soc. (London) A275, 113 (1963).

³R. W. Stark and T. G. Eck, Case Institute of Technology Solid State Physics Progress Report No. AD-298-129, 1963 (unpublished).

⁴F. T. Hedgcock and Y. Muto, Phys. Rev. 134, A1593 (1964).

⁵R. Stevenson, Can. J. Phys. 45, 4115 (1967).

⁶E. S. Borovik, V. B. Volotskaya, and N. Ya. Fogel', Zh. Eksperim. i Teor. Fiz. 45, 46 (1963)[Soviet Phys. JETP 18, 34 (1964)].

⁷Yu. N. Chiang, V. V. Eremenko, and O. G. Shevchenko, Zh. Eksperim. i Teor. Fiz. 57 1923 (1969)[Soviet Phys. JETP 30, 1040 (1970)].

⁸J. M. Ziman, *Electrons and Phonons* (Oxford U. P., London, 1960).

⁹J. C. Garland and R. Bowers, Phys. Rev. 188, 1121 (1969).

¹⁰J. Babiskin and P. G. Siebenmann, Physik Kondensierten Materie 9, 113 (1969).

¹¹R. A. Young, Phys. Rev. 175, 813 (1968).

¹²R. A. Young, Phys. Rev. 183, 611 (1969).

¹³A. B. Pippard, Proc. Roy. Soc. (London) A305, 291 (1968).

¹⁴D. Shoenberg, in *The Physics of Metals*, edited by

J. M. Ziman (Cambridge U. P., Cambridge 1969), p. 97.

¹⁵B. Lüthi, Helv. Phys. Acta. 32, 470 (1959).

¹⁶R. J. Balcombe and R. A. Parker, Phil. Mag. 21, 533 (1970).

¹⁷A. B. Pippard, footnote to R. G. Chambers, in *Solid State Physics: Vol. 1, Electrons in Metals*, edited by J. F. Cochran and R. R. Haering (Gordon and Breach, New York, 1968), p. 319. Also, see H. Stachowiak, Physica 45, 481 (1970).

¹⁸A. F. Clark and F. R. Fickett, Rev. Sci. Instr. 40, 465 (1969).

¹⁹F. R. Fickett and A. F. Clark, J. Appl. Phys. 42, 217 (1971).

²⁰G. T. Meaden, *Electrical Resistance of Metals* (Plenum, New York, 1965).

²¹R. J. Corruccini, Natl. Bur. Std. Technical Note No. 218 (GPO, Washington D. C., 1964).

²²G. Brandli and J. L. Olsen, Mater. Sci. Eng. 4, 61 (1969).

²³V. D. Arp, M. B. Kasen, and R. P. Reed, Air Force Aero Propulsion Laboratory Technical Report No. AFAPL-TR-68-87, 1969 (unpublished).

²⁴F. Pawlek and D. Rogalla, Cryogenics 6, 14 (1966).

²⁵B. N. Aleksandrov, Zh. Eksperim. i Teor. Fiz. 43, 399 (1962)[Soviet Phys. JETP 16, 286 (1963)].

²⁶F. Montariol and R. Reich, Compt. Rend. 254, 3357 (1962).

²⁷J. E. Neighbor and R. S. Newbower, Phys. Rev. 186, 649 (1969).

²⁸N. W. Ashcroft, Physik. Kondensierten Materie 9, 45 (1969).

²⁹F. R. Fickett, A. F. Clark, and R. L. Powell, Bull.

Am. Phys. Soc. 14, 306 (1969).

³⁰R. A. Young, J. Ruvalds, and L. M. Falicov, Phys. Rev. 178, 1043 (1969).

³¹O. P. Katyal and A. N. Gerritsen, Phys. Rev. 178, 1037 (1969).

³²L. M. Falicov and P. R. Sievert, Phys. Rev. 138, A88 (1965).

³³J. Babiskin and P. G. Siebenmann, Naval Research Laboratory Report No. 5949, 1963 (unpublished).

³⁴B. N. Aleksandrov, Zh. Eksperim. i Teor. Fiz. 43,

1231 (1962) [Soviet Phys. JETP 16, 871 (1963)].

³⁵D. H. Damon, M. P. Mathur, and P. G. Klemens, Phys. Rev. 176, 876 (1968).

³⁶J. O. Strom-Olsen, Proc. Roy. Soc. (London) A302, 83 (1967).

³⁷T. Amundsen and P. Seeberg, J. Phys. C 2, 694 (1969).

³⁸T. Amundsen and R. P. Sjøvik, J. Low Temp. Phys. 2, 121 (1970).